TiS Trends in Sciences
TRENDS IN SCIENCES 2027; 24(1): 13978
SPRINT Scholarly Publishing and Repository Integration Center
https://doi.org/10.48048/tis.2027.13978
RESEARCH ARTICLE

Smartphone-Assisted Fluorescence Detection of Histamine Using Chitosan-Derived Graphene Quantum Dots for Food Safety Monitoring

Kittichai Jinachai[1], Jirapatpong Senabut[2], Anusorn Yodjaiphet[3], Sakchai Satienperakul[4] and Mathukorn Sainakham[5,*]

[1]*Chemistry Faculty of Science and Agricultural Technology, Rajamangala University of Technology Lanna, Chiang Mai 50300, Thailand*
[2]*Chemistry Faculty of Science and Agricultural Technology, Rajamangala University of Technology Lanna, Chiang Rai 57120, Thailand*
[3]*Electrical Engineering Faculty of Engineering, Rajamangala University of Technology Lanna, Chiang Rai 57120, Thailand*
[4]*Department of Chemistry, Faculty of Science, Maejo University, Chiang Mai 50290, Thailand*
[5]*Department of Pharmaceutical Sciences, Faculty of Pharmacy, Chiang Mai University, Chiang Mai 50200, Thailand*

([*]Corresponding author's e-mail: mathukorn.s@cmu.ac.th)

Received: 3 April 2026, Revised: 7 June 2026, Accepted: 17 June 2026, Published: 5 August 2026

Abstract

This research aimed to develop a smartphone-assisted fluorescence sensing platform for rapid histamine detection using graphene quantum dots (GQDs) synthesized from chitosan precursor via a hydrothermal carbonization process. The synthesized GQDs, with particle sizes ranging from 2 to 6 nm, exhibited fluorescence quenching behavior upon interaction with histamine, possibly associated with Schiff-base formation and aggregation-related effects. The sensing platform demonstrated selective fluorescence response toward histamine in the presence of common ionic interferents, including sodium and magnesium ions at concentrations up to 1,000-fold higher. Histamine detection was evaluated within the concentration range of 0.25 - 0.75 mM using fluorescence intensity and smartphone-assisted RGB analysis under controlled imaging conditions. The proposed platform offers a simple, low-cost, portable, and user-friendly approach with promising potential for rapid preliminary food quality screening and onsite monitoring applications.

Keyword: Graphene quantum dots, Histamine, Fluorescence sensing, Smartphone-Assisted detection, RGB analysis

Introduction

Histamine is a biogenic amine commonly found in food products and beverages, particularly in fish products, fermented foods, dairy products, meat products, soy-based products, and alcoholic beverages. It is primarily generated through the decarboxylation of the amino acid histidine, often associated with microbial activity during food processing and storage [1,2]. Although histamine naturally occurs in certain foods, excessive accumulation may lead to adverse health effects, including food poisoning, headache, nausea, flushing, hypotension, and allergic-like symptoms [3]. Due to these potential health risks, many countries and international organizations have established regulatory limits for histamine levels in food products, especially in seafood and fermented products, to ensure consumer safety and maintain product quality [4,5].

Currently, histamine analysis in food samples is commonly performed using chromatographic techniques such as High-Performance Liquid Chromatography (HPLC), owing to their high analytical accuracy and sensitivity [6]. However, these methods generally require expensive instrumentation, derivatization procedures, complicated sample preparation, and skilled operators, which may limit their

applicability for rapid onsite screening and routine monitoring applications [7]. Consequently, increasing attention has been directed toward the development of portable, low-cost, and user-friendly sensing platforms for preliminary food quality assessment.

Among various sensing materials, graphene quantum dots (GQDs) have attracted considerable interest due to their unique fluorescence properties, low toxicity, facile synthesis, and tunable surface functionalities [8]. In addition, chitosan has emerged as an attractive carbon precursor for GQD synthesis because of its biodegradability, availability, and abundant functional groups that may contribute to fluorescence-related interactions [9]. Recent advances in smartphone-assisted sensing technologies and RGB-based image analysis have further expanded the potential for developing portable fluorescence detection systems suitable for rapid analytical applications [10].

Therefore, this research aimed to develop a smartphone-assisted fluorescence sensing platform for histamine monitoring using chitosan-derived graphene quantum dots synthesized through a hydrothermal carbonization process. The study also focused on optimizing experimental conditions for fluorescence detection and smartphone-based RGB analysis to establish a simple, rapid, and cost-effective preliminary screening approach for potential food safety monitoring applications.

Materials and methods

Materials

Acetic acid and polyethylene glycol (PEG) were purchased from Merck (Darmstadt, Germany). Chitosan, glutaraldehyde, histamine dihydrochloride, magnesium chloride, and sodium hydrogen phosphate were obtained from Sigma (St. Louis, MO, USA). Methanol was supplied by Fisher Scientific (Thermo Fisher Scientific Incorporation, USA). Sodium dihydrogen orthophosphate, sodium chloride, and sodium hydroxide were procured from Ajax Chemical (Ajax Finechem, Australia). These reagents were selected based on their common applications in fluorescence-related carbon nanomaterial synthesis and analytical sensing systems [9].

Synthesis of Graphene Quantum Dots (GQDs)

Graphene quantum dots (GQDs) were synthesized in situ from chitosan precursor through a hydrothermal carbonization process. Briefly, 4.5 mL of 2% (v/v) chitosan gel was transferred into a 50 mL Erlenmeyer flask, followed by the addition of 4.5 mL of 25% (v/v) polyethylene glycol (PEG). Subsequently, 1 mL of 5 M sodium hydroxide solution was added to obtain a homogeneous chitosan–PEG–NaOH precursor mixture. The mixture was continuously stirred using a magnetic stirrer for 30 min prior to thermal treatment.

The prepared precursor solution was then transferred into a round-bottom flask connected to the synthesis apparatus illustrated in **Figure 1** and heated at 190 °C for 3 h under oxygen-limited conditions. After naturally cooling to room temperature, 15 mL of deionized water was added to the reaction mixture [10]. The obtained suspension was filtered through a 0.2-µm membrane filter to remove large particulates prior to purification.

The filtrate was subsequently centrifuged at 20,000 rpm for 1 h. After centrifugation, the supernatant containing dispersed GQDs was collected and stored for further characterization and fluorescence sensing experiments. The overall synthesis and purification process is summarized in **Figure 2**.

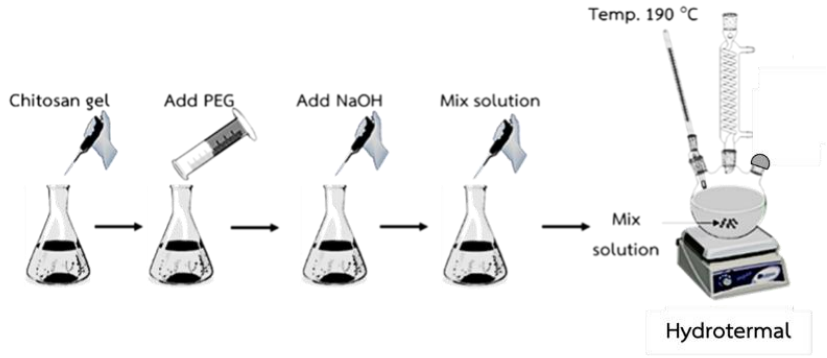


Figure 1 Schematic representation of the thermal synthesis setup used to prepare chitosan-derived graphene quantum dots (GQDs). The configuration illustrates the controlled reaction environment required for precursor carbonization and subsequent formation of fluorescent carbon nanostructures for optical sensing applications.

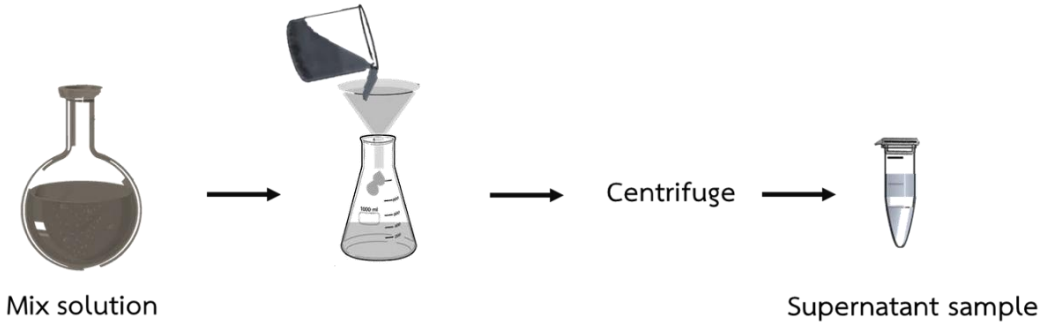


Figure 2 Schematic representation of the purification workflow for chitosan-derived graphene quantum dots (GQDs). The process yields a clarified fluorescent GQD dispersion suitable for physicochemical characterization and smartphone-assisted histamine sensing.

Preparation of standard GQD optical solutions

The synthesized GQDs were dispersed in phosphate buffer solutions at pH values of 6.8, 7.0, 7.2, 7.4, and 7.8. The suspensions were mixed until homogeneous prior to fluorescence measurements and subsequently used as standard optical solutions for histamine sensing studies [11].

Structural characterization of GQDs

The morphology and particle size distribution of the synthesized GQDs were investigated using transmission electron microscopy (TEM) (JEM 2010, USA). Prior to imaging, the nanoparticles were dispersed in ethanol using ultrasonication. A drop of the suspension was deposited onto a 200-mesh carbon-coated copper grid and air-dried before analysis. TEM images were recorded at an accelerating voltage of 200 kV.

Fourier-transform infrared spectroscopy equipped with attenuated total reflectance (FTIR–ATR) (Perkin Elmer, UK) was employed to investigate the surface functional groups of the synthesized GQDs within the spectral range of 600 - 4,000 cm^{-1}. Fluorescence emission characteristics were examined using a fluorescence spectrophotometer (Agilent, USA) in the emission wavelength range of 400 - 600 nm.

Optimization of sensing conditions for histamine detection

Optimization studies were performed to evaluate the influence of GQD concentration, buffer pH, buffer concentration, and histamine concentration on fluorescence response behavior.

Optimization of GQD concentration

For GQD concentration optimization, GQD solutions at concentrations of 0.0, 0.1, 0.3, 0.5, and 0.7

mM were prepared in 0.10 M phosphate buffer (pH 7.0) with a total volume of 5.0 mL. Subsequently, 50 µL of 0.5 mM histamine solution was added prior to fluorescence measurement [12].

Optimization of buffer pH

To investigate the effect of pH, phosphate buffer solutions at pH 6.8, 7.0, 7.2, 7.4, and 7.8 containing 0.50 mM GQDs were prepared. Histamine solution (50 µL, 0.5 mM) was then added before fluorescence analysis [10].

Optimization of buffer concentration

The effect of buffer concentration was studied using phosphate buffer concentrations of 0.10, 0.50, 0.80, and 1.0 M containing 0.50 mM GQDs. Histamine solution (50 µL, 0.5 mM) was added prior to fluorescence measurements [11].

Optimization of histamine concentration

For histamine concentration optimization, histamine solutions at concentrations of 0.25, 0.50, 0.75, and 1.0 mM were prepared using 0.50 mM GQDs dispersed in 0.10 M phosphate buffer (pH 7.2) [7].

Interference study

Interference experiments were conducted using 0.70 mM GQDs dispersed in 0.10 M phosphate buffer (pH 7.2) containing 0.5 mM histamine. The analyte-to-interferent ratios ranged from 1:1 to 1:1,000. Sodium chloride and magnesium chloride were selected as representative ionic interferents to preliminarily evaluate fluorescence selectivity behavior [9].

Linearity and smartphone-assisted RGB analysis

Standard histamine solutions at concentrations of 0.00, 0.25, 0.50, and 0.75 mM were prepared to evaluate the linear relationship between histamine concentration and fluorescence response using smartphone-assisted RGB analysis.

Fluorescence images were acquired under controlled imaging conditions using an enclosed dark box to minimize ambient light interference. A fixed imaging distance was maintained between the smartphone camera and the sample holder throughout image acquisition. Exposure and white balance settings were locked prior to image collection to reduce automatic brightness adjustment during fluorescence measurements. RGB intensity values were analyzed using the RGB Detector application by selecting regions of interest (ROI) corresponding to the fluorescence emission area.

Results and discussion

Physical and structural characterization of GQD

Particle size analysis of GQD using TEM

Figure 3 illustrate the synthesized graphene quantum dots (GQDs) obtained from chitosan precursor through hydrothermal carbonization, appearing as a yellowish powder after purification. Transmission electron microscopy (TEM) analysis revealed semi-spherical nanoparticles with particle sizes ranging from 2 - 6 nm and a relatively broad size distribution. The formation of nanoscale carbon domains within this size range is consistent with the successful generation of graphene quantum dots via a bottom-up carbonization approach [12-14].

The observed fluorescence properties of the synthesized GQDs are likely associated with quantum confinement effects and surface-state emissions commonly reported in carbon-based quantum nanomaterials [18,19,21]. Although some degree of polydispersity was observed, such variation is frequently encountered in biomass-derived GQDs synthesized through thermal carbonization processes [15-17]. The relatively broad particle size distribution may contribute to heterogeneous surface energy states and multiple emissive sites, which can influence fluorescence behavior and analyte interaction sensitivity [10,18].

Furthermore, the utilization of chitosan as a precursor supports the development of environmentally friendly carbon nanomaterials due to its biodegradability, biocompatibility, and renewable origin [15,17]. This approach also aligns with current trends in sustainable nanomaterial synthesis using biomass-derived carbon sources [14-17].

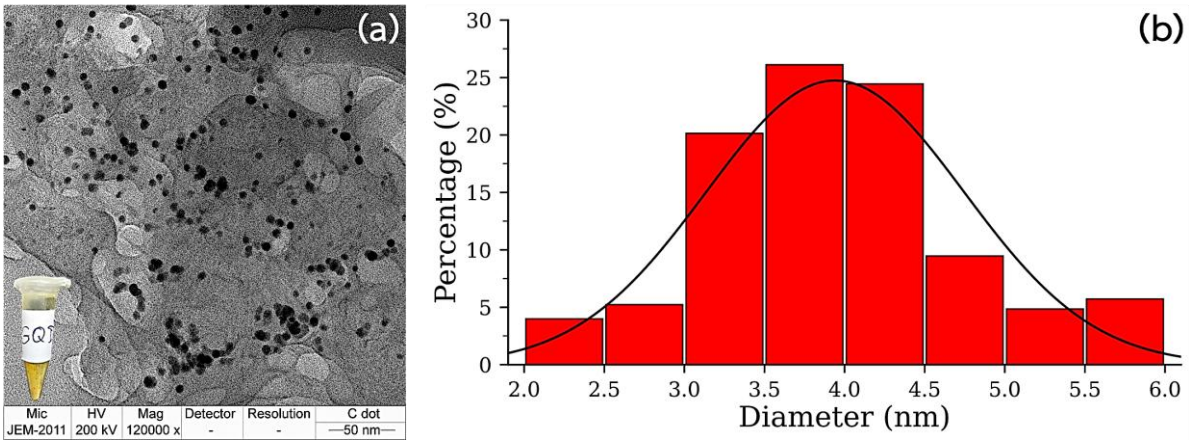


Figure 3 Morphological and size-distribution analysis of the synthesized chitosan-derived graphene quantum dots (GQDs). (a) TEM image showing nanoscale, semi-spherical GQD particles and (b) the particle-size distribution histogram.

Functional group analysis of GQD using FTIR

Figure 4 presents the FTIR spectrum of the synthesized GQDs in the range of 600 - 4,000 cm^{-1}. The broad absorption peak observed at approximately 3,356 cm^{-1} corresponds to O–H stretching vibrations, while the peak around 1,700 cm^{-1} is attributed to C=O stretching of carboxylic groups. Peaks located at 1,435 and 1,396 cm^{-1} are associated with C–O–C functional groups, whereas the signal at 1,212 cm^{-1} corresponds to C=C stretching vibrations. In addition, the peaks at 2,895 and 746 cm^{-1} can be assigned to C–H stretching and C=C bending vibrations, respectively.

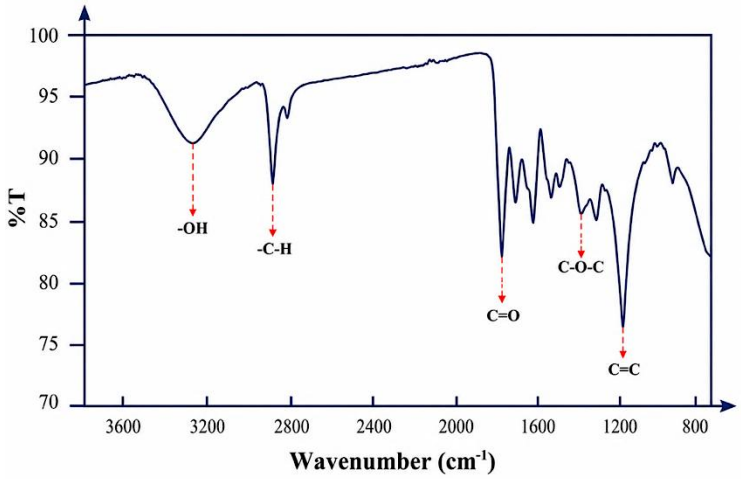


Figure 4 FTIR spectra of the GQD functional groups in the wavenumber range of 600 - 4,000 cm^{-1}.

The presence of oxygen-containing functional groups such as hydroxyl, carbonyl, and ether groups indicates that the synthesized GQDs possess hydrophilic surface characteristics and favorable water dispersibility [18,19]. These surface functional groups may also provide active interaction sites for histamine molecules through hydrogen bonding or Schiff-base-related interactions involving amino-containing compounds [20,41,42].

In addition to improving aqueous stability, the surface oxygen functionalities are believed to play an important role in fluorescence behavior by generating surface-state emissive sites within the carbon nanostructure [10,18,21]. Such chemically active surfaces may contribute to fluorescence response changes after interaction with histamine molecules.

Fluorescence emission spectroscopy analysis of GQD

Figure 5 shows the fluorescence emission spectrum of the synthesized GQDs. A strong excitation feature was observed around 360 - 370 nm, which is commonly associated with π–π* electronic transitions of sp^2-hybridized carbon domains within graphene-based nanostructures [18,21]. The emission spectrum exhibited a broad fluorescence band centered near 450 nm, corresponding to blue fluorescence emission from surface-state-related energy levels [10,21].

The broad emission behavior observed within the 400 - 550 nm range may be attributed to heterogeneous surface energy distributions and multiple radiative recombination pathways arising from oxygen-containing functional groups and structural defects [10,18,25]. Similar fluorescence characteristics have been widely reported for carbon quantum dots synthesized from biomass-derived precursors [15,17].

The fluorescence response of GQDs is highly sensitive to changes in the surrounding chemical environment. Interaction between histamine molecules and surface functional groups on GQDs may alter electron transfer pathways and surface-state relaxation processes, resulting in fluorescence quenching behavior [7,20,32,33]. This fluorescence response provides the basis for the proposed histamine sensing platform developed in this study.

In addition, the fluorescence emission characteristics were visually observable under LED excitation, supporting the feasibility of smartphone-assisted RGB monitoring for preliminary fluorescence signal analysis [8,34-40].

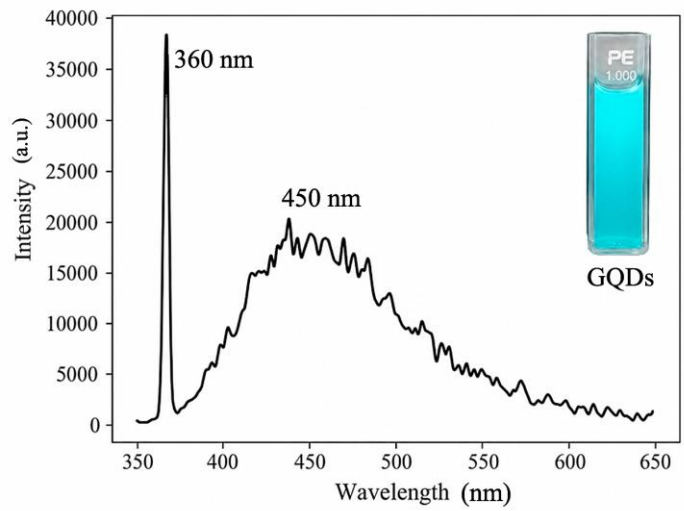


Figure 5 UV–Vis absorption and fluorescence emission spectra of the synthesized chitosan-derived graphene quantum dots (GQDs). The absorption indicates blue-emission carbon nanostructures for smartphone-assisted histamine sensor.

RGB color analysis of GQD solutions

The RGB color values of GQD solutions prepared in phosphate buffer were analyzed using a smartphone-assisted RGB detection application under controlled imaging conditions. Fluorescence images were acquired inside a dark box under 450 nm LED excitation while maintaining a fixed imaging distance between the smartphone camera and sample holder. Exposure and white balance settings were locked prior to image acquisition to minimize automatic image adjustment during fluorescence measurement. All measurements were performed in triplicate (n = 3), and the results are presented as mean ± standard deviation (SD).

As summarized in **Table 1**, the synthesized GQDs exhibited blue fluorescence emission, corresponding primarily to strong blue-channel intensity values within the RGB analysis system. The observed fluorescence behavior is consistent with the emission characteristics of carbon-based quantum dots reported in previous studies [18,21].

Changes in RGB intensity and B/R ratio may reflect alterations in fluorescence emission behavior caused by histamine interaction with the GQD surface

[34-40]. The fluorescence quenching effect observed after histamine addition suggests possible modification of surface-state electron relaxation pathways and intermolecular interactions between histamine molecules and oxygen-containing functional groups on the GQD surface [20,32,33].

The smartphone-assisted RGB approach provides a simple and low-cost preliminary fluorescence monitoring platform that may support portable food safety screening applications. Although the present study primarily demonstrates proof-of-concept feasibility, the results suggest the potential applicability of smartphone-assisted fluorescence monitoring systems for rapid on-site analytical screening [8,35-40].

Table 1 Histamine concentrations and fluorescence responses obtained by RGB and fluorescence spectroscopy (FL). Values are presented as mean ± SD (n = 3).

Histamine concentration (mM)	RGB Method							FL Method		
	Mean (R)	SD	Mean (G)	SD	Mean (B)	SD	B/R	Mean	SD	(F_0/F)
0.00	1.29	±0.01	136.0	±0.70	256.6	±0.80	198.9	259.6	±1.35	1.000
0.25	1.27	±0.01	133.0	±0.70	249.3	±0.90	196.3	246.2	±1.65	1.055
0.50	1.24	±0.01	131.4	±0.80	216.5	±1.20	174.6	214.6	±1.80	1.210
0.75	1.21	±0.01	128.6	±0.85	199.3	±1.20	164.7	195.8	±1.70	1.326

Optimization of GQD conditions for histamine detection

Optimization of GQD concentration

Figure 6 demonstrates that the fluorescence intensity of the GQD solution increased progressively with increasing GQD concentration and reached a maximum response at 0.5 mM. This concentration was therefore selected as the optimal condition for subsequent experiments. The enhanced fluorescence signal at moderate concentrations may be attributed to the increased availability of emissive surface states and improved interaction probability between excitation energy and fluorescent domains within the GQDs [10,18].

However, when the concentration exceeded 0.5 mM, a reduction in fluorescence intensity was observed. This behavior is likely associated with aggregation-induced quenching (ACQ) and inner filter effects (IFE), which commonly occur in highly concentrated fluorescent nanomaterial systems [23-25]. At elevated concentrations, the planar structure of graphene-based nanomaterials may promote π–π stacking interactions, leading to particle aggregation and reduced radiative recombination efficiency [13,25,26].

In addition, increased solution viscosity at higher GQD concentrations may restrict particle dispersion and alter fluorescence emission behavior. These findings indicate that controlling GQD concentration is critical for maintaining colloidal stability and maximizing fluorescence response during histamine sensing applications.

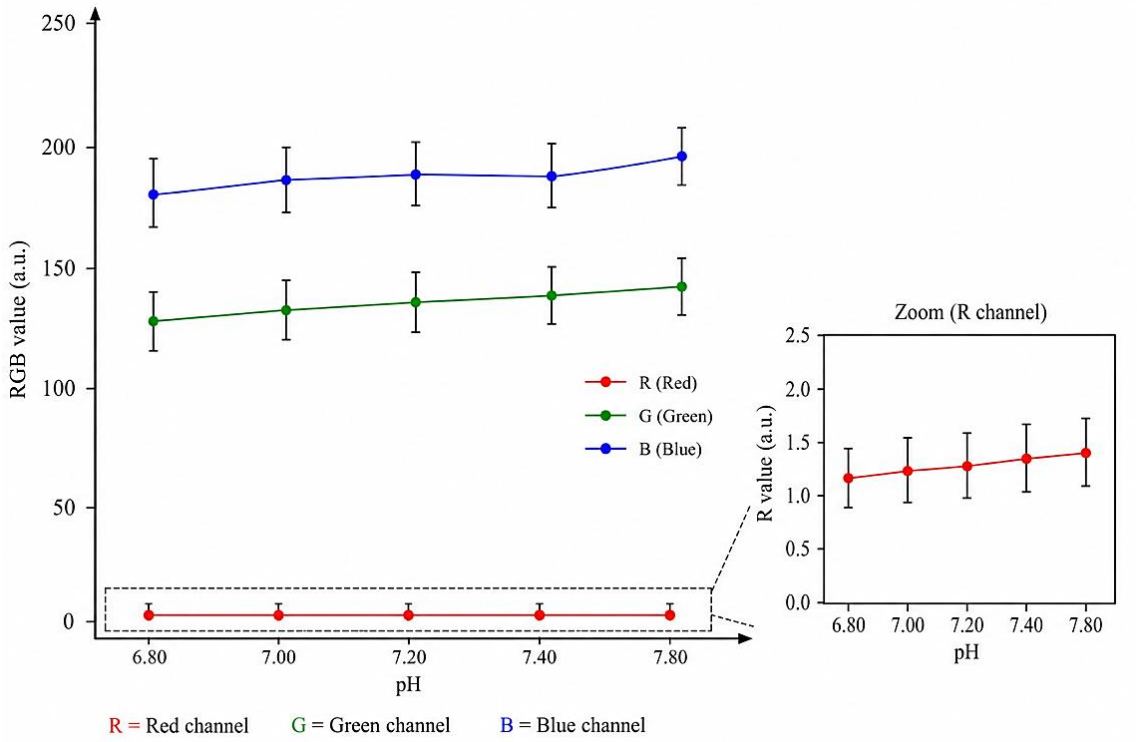


Figure 6 Effect of GQD concentration on blue light intensity under experimental conditions containing 5.0 mL of phosphate buffer at pH 7.0 and 50 µL of 0.5 mM histamine

Optimization of buffer pH

Figure 7 shows that buffer pH significantly affected the fluorescence behavior of the synthesized GQDs. The fluorescence intensity gradually increased under near-neutral conditions and reached the highest response at approximately pH 7.0 - 7.2. This behavior may be associated with improved colloidal stability and reduced particle aggregation under optimal protonation conditions [18,28].

The fluorescence properties of GQDs are strongly influenced by protonation and deprotonation processes occurring on oxygen-containing functional groups such as carboxyl and hydroxyl groups located on the particle surface [18]. Under highly acidic conditions, protonation reduces negative surface charge density and electrostatic repulsion between particles, thereby promoting aggregation and fluorescence quenching [13,27].

Conversely, near-neutral pH conditions enhance particle dispersion and stabilize surface-state emissive sites, resulting in improved fluorescence emission efficiency [10,18,26]. In addition, pH variation may influence hydrogen bonding interactions between histamine molecules and the GQD surface, which can further affect fluorescence response behavior during sensing measurements [20,41,42].

These observations are consistent with previously reported surface-state emission mechanisms in carbon-based quantum nanomaterials, in which surface chemistry and environmental conditions strongly influence fluorescence performance [10,21,26].

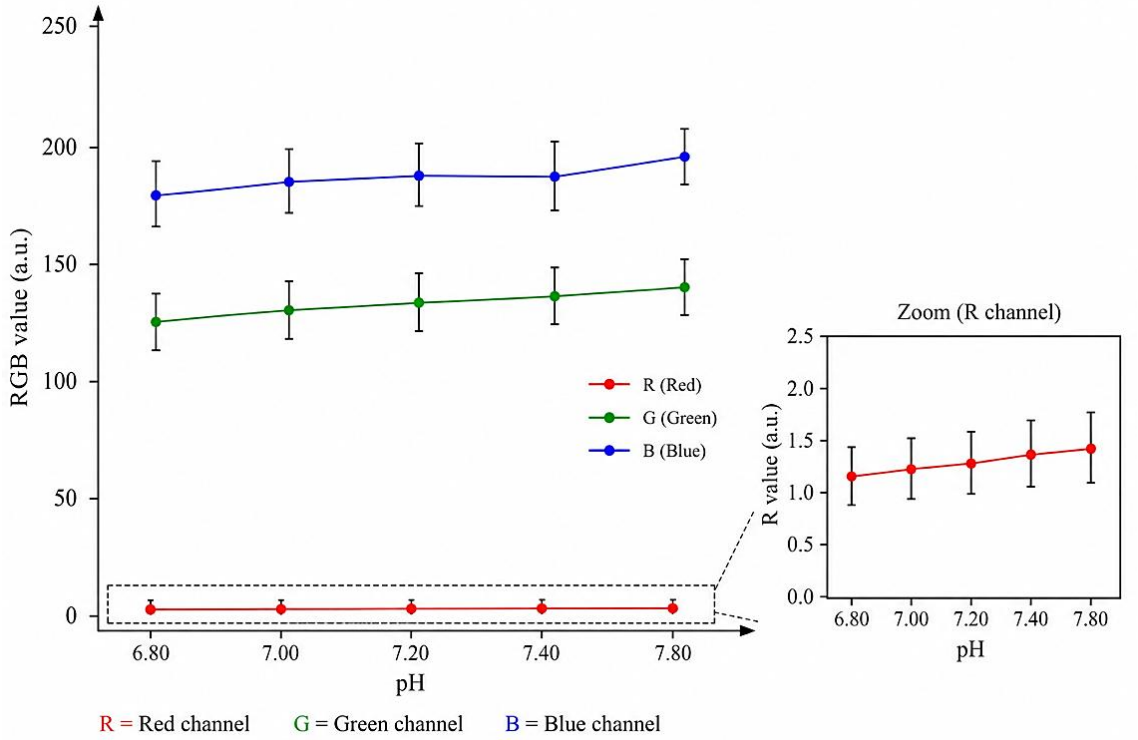


Figure 7 Effect of buffer pH on blue light intensity under experimental conditions containing 5.0 mL of 0.50 mM GQD and 50 µL of 0.5 mM histamine.

Optimization of buffer concentration

The effect of buffer concentration on fluorescence behavior is presented in **Figure 8**. The results showed that excessive buffer concentrations negatively affected fluorescence intensity and signal stability. Increased ionic strength may interfere with colloidal stability and alter particle interactions within the GQD suspension [28,29].

This phenomenon is likely caused by charge screening effects on the GQD surface. At elevated ionic strengths, electrostatic repulsion between particles decreases, resulting in increased aggregation tendency and fluorescence quenching [28,29]. Such aggregation may disrupt surface-state emission pathways and reduce fluorescence efficiency.

Furthermore, highly concentrated buffer systems may influence intermolecular interactions and potentially induce undesirable side effects within the sensing environment [30]. Therefore, careful optimization of buffer concentration is essential to maintain fluorescence stability, minimize aggregation effects, and improve sensing reproducibility.

These findings are particularly important for the future development of practical fluorescence-based sensing platforms and portable test kits, where environmental stability and reproducibility are critical factors.

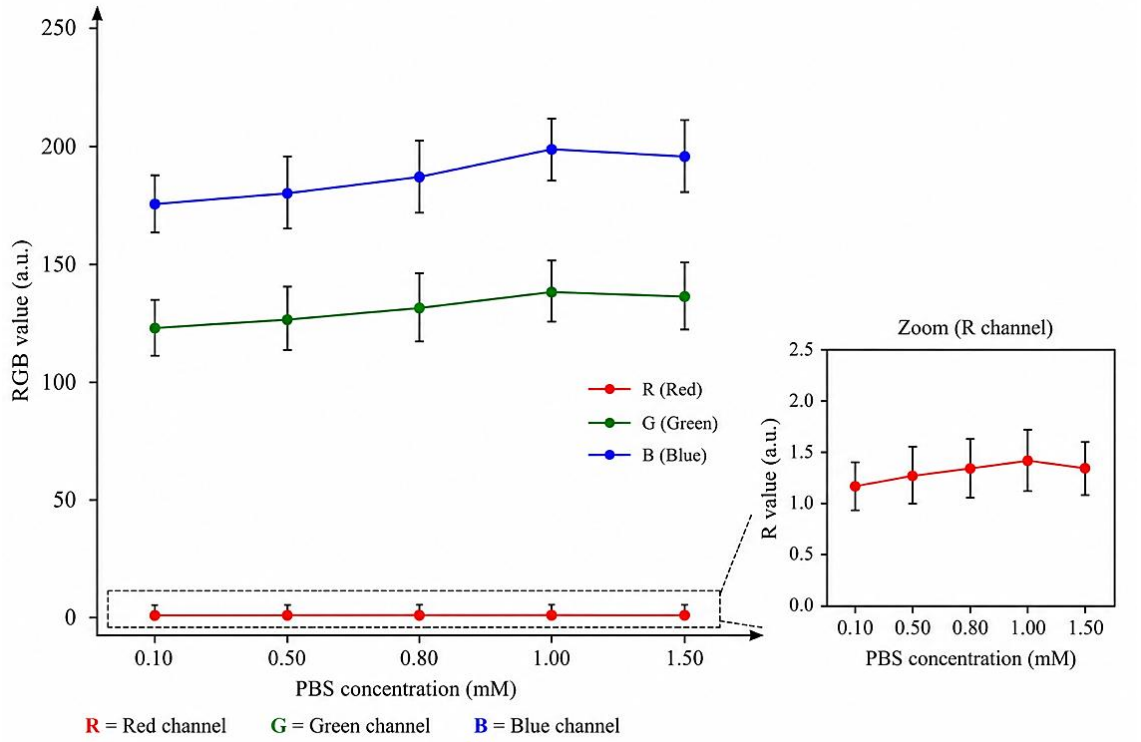


Figure 8 Effect of buffer concentration on blue light intensity under experimental conditions containing 5.0 mL of 0.50 mM GQD and 50 µL of 0.5 mM histamine.

Optimization of histamine concentration

Figure 9 presents the fluorescence response of GQDs toward different histamine concentrations. Within the investigated concentration range, only minor changes in fluorescence intensity were observed. This behavior suggests that the interaction between histamine molecules and the GQD surface may remain limited at lower concentration levels [7,11].

The relatively stable fluorescence response observed at low histamine concentrations may indicate the presence of a threshold effect associated with the lower detection capability of the sensing system [11,31]. In addition, the high colloidal stability and structural robustness of the synthesized GQDs may contribute to resistance against weak environmental perturbations and minor background interference [7].

Although the fluorescence response remained relatively stable at lower concentrations, slight fluorescence quenching behavior was still observable, which may be associated with partial electron transfer interactions or surface-state modifications induced by histamine adsorption on the GQD surface [20,32,33].

These results suggest that further surface engineering or functional modification of GQDs may be beneficial for improving sensitivity toward trace-level histamine detection. Nevertheless, the current platform demonstrates promising preliminary performance for smartphone-assisted fluorescence monitoring applications.

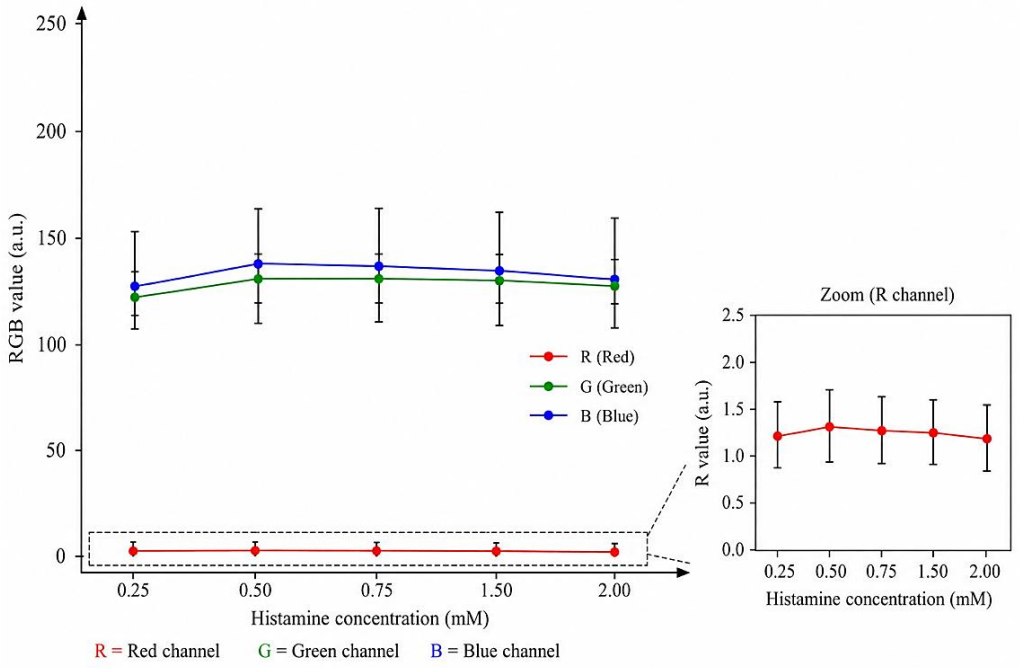


Figure 9 Effect of histamine concentration on blue light intensity under experimental conditions containing 5.0 mL of 0.50 mM GQD in 0.10 M phosphate buffer at pH 7.4

RGB color analysis of GQD solutions

The interference effects of sodium chloride (NaCl) and magnesium chloride ($MgCl_2$) on the fluorescence response of the GQD sensing platform were investigated to evaluate the selectivity and robustness of the proposed system under conditions relevant to real food matrices. As shown in **Figure 10**, the blue-channel intensity (B value) remained relatively stable in the presence of both Na^+ and Mg^{2+} ions over interference ratios ranging from 1-fold to 1,000-fold relative to histamine concentration. The fluorescence variation remained within approximately ±10%, indicating that common ionic species produced only minor changes in the optical response of the GQDs toward histamine detection. These findings suggest that the sensing behavior was not dominated by nonspecific ionic interactions, but was more likely associated with selective interactions occurring between histamine molecules and reactive surface functional groups on the GQDs [7,9,32,33].

The observed tolerance toward high ionic strength environments is particularly important for practical food-analysis applications, especially in fermented foods and seafood products where sodium and magnesium ions are naturally abundant. In many fluorescence-based nanomaterial systems, dissolved ions may induce fluorescence quenching through aggregation, charge screening, or surface-state disruption. However, the synthesized GQDs in this study maintained relatively stable fluorescence behavior even under elevated ionic conditions, suggesting satisfactory colloidal stability of the sensing platform. This stability may be attributed to the presence of oxygen-containing functional groups on the GQD surface, which help maintain particle dispersion and reduce undesirable aggregation effects [18,28,29].

In addition, the relatively stable RGB response obtained from the smartphone-assisted analysis indicates that the proposed sensing platform may be suitable for preliminary onsite screening applications where environmental conditions cannot be strictly controlled. Nevertheless, additional interference studies involving more complex food matrices, amino acids, and biogenic amines may further strengthen the selectivity assessment of the proposed platform in future investigations [11,35,39].

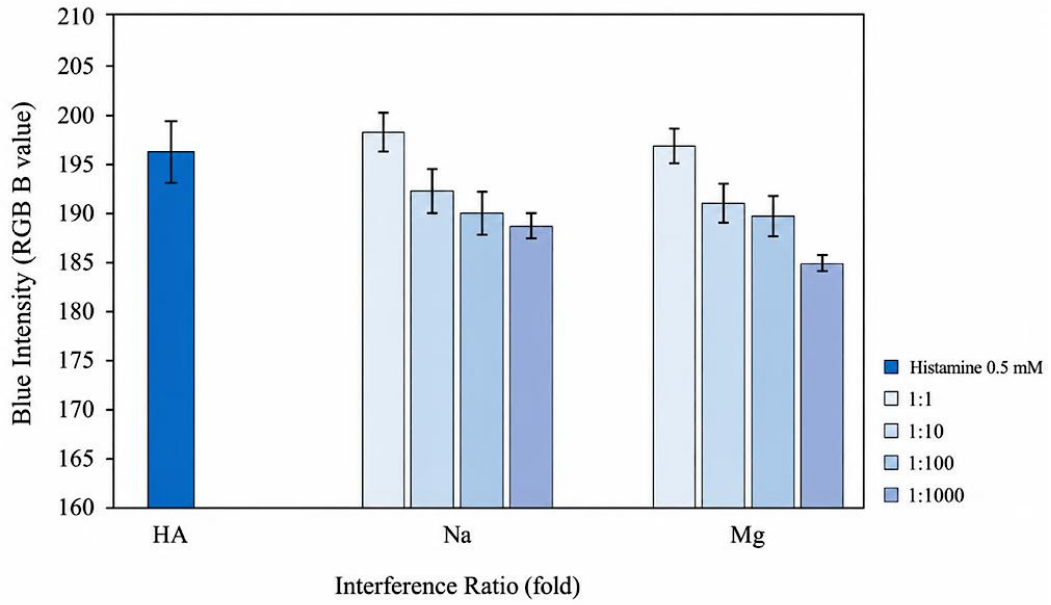


Figure 10 Effect of interfering ions from NaCl and $MgCl_2$ with interferent-to-analyte ratios ranging from 1 to 1,000 on the measurement signal under conditions of GQD 0.70 mM in 0.10 M phosphate buffer at pH 7.2 and 0.5 mM histamine.

Linearity of histamine detection

The linearity of the proposed smartphone-assisted fluorescence sensing platform was evaluated using histamine standard solutions in the concentration range of 0.00 - 0.75 mM. The corresponding fluorescence responses were quantified using the blue-channel (B) intensity obtained from RGB image analysis, as summarized in **Table 2** and **Figure 11**. A concentration-dependent fluorescence response was observed within the investigated range, indicating that histamine concentration influenced the optical behavior of the GQD system [7,11].

The linear regression equation obtained from the calibration curve was:

$$y = –81.88x + 261.13$$

with a correlation coefficient (R^2) of 0.9506, demonstrating good linearity between histamine concentration and fluorescence response. The relatively high correlation coefficient suggests that the smartphone-assisted RGB analysis approach may provide reliable semi-quantitative monitoring capability within the tested concentration range [34-38].

Rather than indicating a strong fluorescence enhancement mechanism alone, the observed optical response may be associated with changes in surface-state interactions occurring between histamine molecules and functional groups present on the GQD surface. Variations in electron distribution, hydrogen bonding interactions, and localized surface-state modulation may contribute to the observed fluorescence behavior. Such interactions are commonly reported in carbon-dot-based sensing systems involving amine-containing analytes [9,10,20,42].

Table 2 LOD of histamine concentration.

Method	LOD (mM)	LOQ (mM)
B intensity	0.806	2.443
B/R ratio	0.796	2.414
FL method	0.052	0.158

Although the present study demonstrated promising linearity under controlled laboratory conditions, the platform should currently be regarded as a preliminary fluorescence screening approach rather than a replacement for conventional quantitative analytical instrumentation such as HPLC. Further optimization, replicate validation, and real-sample analysis are still required to fully establish analytical performance parameters including LOD, LOQ, reproducibility, and long-term stability [6,8,35].

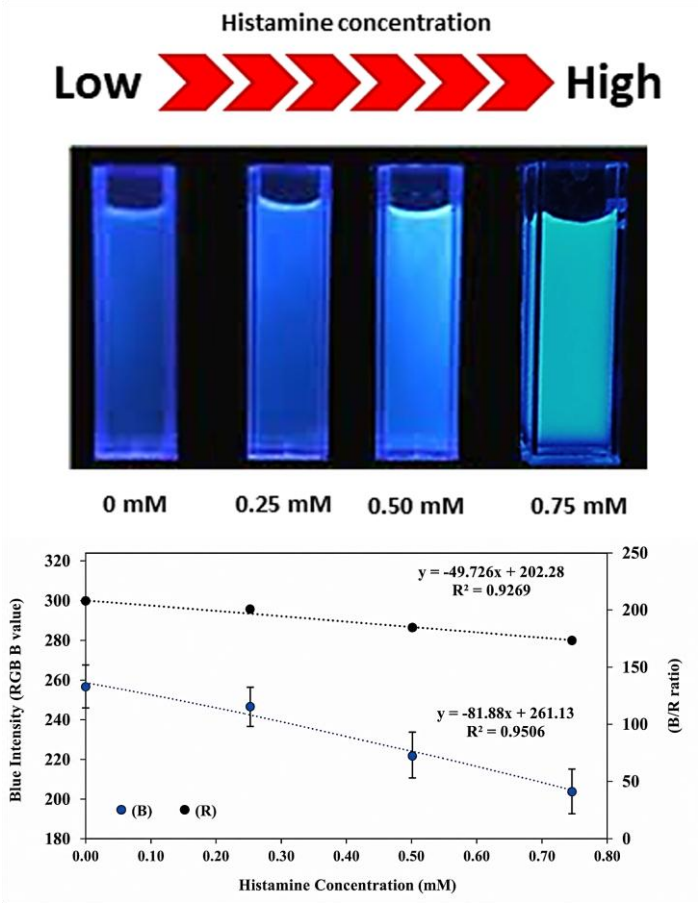


Figure 11 Linear relationship between histamine concentration and blue channel intensity in quenching mode. The fluorescence intensity decreased linearly with increasing histamine concentration, indicating a quenching-dominated sensing mechanism.

Smartphone-assisted RGB detection procedure

Figure 12 illustrates the workflow used for smartphone-assisted fluorescence analysis of histamine solutions using the RGB Color Detector application. Histamine solutions with different concentrations were placed in cuvettes and illuminated using a 360 nm LED excitation source inside a dark enclosure to minimize ambient light interference. The emitted fluorescence images were captured using an Android smartphone positioned at a fixed distance from the sample holder to maintain imaging consistency [34-40].

To minimize signal variation caused by automatic camera adjustment, exposure and white-balance settings were locked prior to image acquisition. The smartphone application was configured to analyze fluorescence intensity from selected regions of interest (ROI) corresponding to the emission area of the GQD solution. RGB values were subsequently extracted and used for semi-quantitative fluorescence analysis [35,36,40].

This imaging strategy provides a low-cost and user-friendly alternative for fluorescence monitoring without requiring complex optical instrumentation. However, fluorescence intensity may still be influenced by factors such as camera sensitivity, LED intensity variation, ROI selection, and environmental conditions. Therefore, standardized imaging conditions remain important for improving analytical reproducibility [34,37,38].



Figure 12 Smartphone-assisted RGB analysis for evaluating fluorescence responses of GQD–histamine solutions. Fluorescence images of histamine standard solutions were captured under controlled imaging conditions and analyzed using the RGB Color Detector application to quantify changes in blue-channel intensity.

Design of a smartphone-integrated device for histamine quantification

A smartphone-assisted fluorescence detection platform was developed using a custom-designed 3D-printed enclosure integrated with LED excitation and RGB image analysis. The system was designed to provide controlled optical conditions for fluorescence monitoring while maintaining low fabrication cost and operational simplicity. **Figure 13** illustrates the structural design and practical implementation of the sensing platform [34-39].

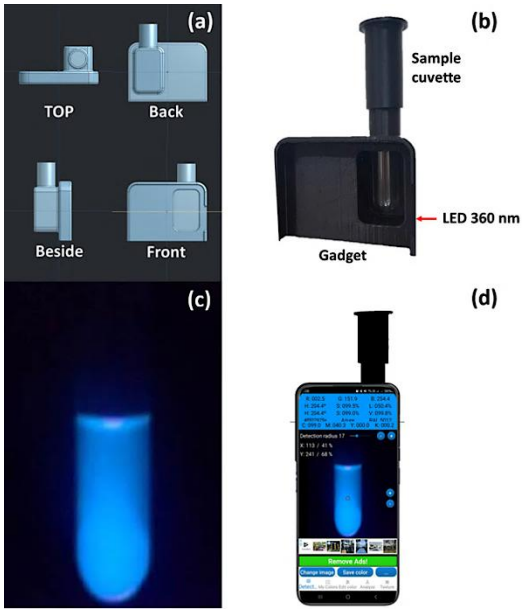


Figure 13 Design of the optical detection platform utilizing 3D modeling: (a) 3D printed housing, (b) components of the detection platform, (c) photograph of GQD solution captured by smartphone and (d) RGB based mobile application.

The enclosure was designed to minimize external light interference and maintain a fixed spatial arrangement between the excitation source, sample holder, and smartphone camera. A 360 nm LED was used as the excitation source to stimulate fluorescence emission from the GQD solution. Under UV excitation, the GQD solution emitted visible blue fluorescence,

which was subsequently captured using a smartphone camera for RGB analysis [18,21,34].

The integration of smartphone imaging with a portable optical enclosure represents a practical approach for preliminary point-of-care and onsite fluorescence screening applications. Compared with conventional fluorescence instrumentation, smartphone-assisted systems offer advantages including portability, reduced cost, simplified operation, and accessibility for non-specialized users. These characteristics support the growing interest in smartphone-based analytical sensing platforms for food-quality monitoring and decentralized analysis [8,34-39].

To improve measurement consistency, fluorescence imaging was performed under controlled conditions including fixed imaging distance, dark-box operation, and locked camera exposure settings. The RGB Detector application was used to extract color intensity values from selected regions of interest (ROI). This approach helped reduce variability associated with automatic image processing and ambient illumination changes [35,36,40].

Proposed interaction mechanism between histamine and GQDs

Figure 14 schematically illustrates the proposed interaction pathway between histamine molecules and oxygen-containing functional groups located on the GQD surface. Histamine contains primary amine functionalities that may interact with carbonyl- or aldehyde-related surface groups through Schiff-base-related interactions or hydrogen bonding processes. These interactions can alter the local electronic environment of the GQDs and subsequently influence fluorescence emission behavior [20,41,42].

In the present study, the sensing mechanism was interpreted primarily in terms of fluorescence quenching behavior to maintain consistency throughout the manuscript. The observed fluorescence variation may be associated with surface-state modulation, electron-transfer processes, or localized aggregation effects induced by histamine interaction with the GQD surface. Similar fluorescence-response mechanisms have been reported in carbon-dot-based sensing systems involving amine-containing analytes [9,10,31,42].

Rather than claiming a fully confirmed mechanistic pathway, the proposed interaction mechanism should currently be regarded as a plausible interpretation based on fluorescence behavior and FTIR observations. Additional mechanistic investigations such as time-resolved fluorescence analysis, zeta-potential measurements, or surface-state characterization may be required to fully validate the interaction pathway in future studies [10,28,43].

The combination of smartphone-assisted RGB analysis with fluorescence-responsive GQDs demonstrates the potential of the proposed platform as a low-cost preliminary screening tool for histamine monitoring in food products. However, further validation using real food samples and replicate experiments remains necessary before practical implementation in routine analytical applications [8,11,35].

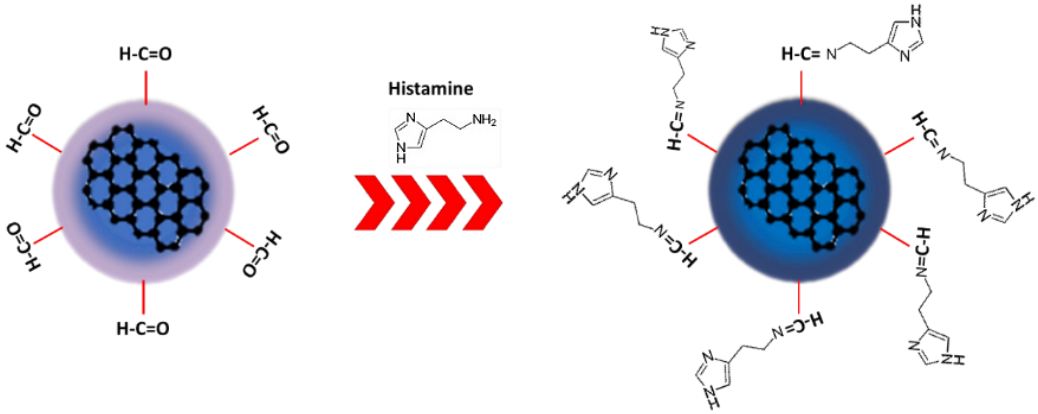


Figure 14 Proposed interaction mechanism between histamine and chitosan-derived graphene quantum dots (GQDs). Histamine may interact with oxygen-containing surface functional groups on the GQDs through Schiff-base-related interactions and hydrogen bonding, resulting in changes in fluorescence behavior.

Conclusions

This study demonstrated the successful synthesis of graphene quantum dots (GQDs) derived from chitosan precursor materials through a hydrothermal carbonization process for potential application in smartphone-assisted histamine monitoring. The synthesized GQDs exhibited quasi-spherical morphology with particle sizes ranging from 2 - 6 nm and showed oxygen-containing surface functional groups that contributed to good aqueous dispersibility and fluorescence responsiveness. FTIR and fluorescence analyses suggested that the surface-state properties of the GQDs played an important role in the interaction behavior toward histamine molecules [9,10,18,20].

Optimization studies indicated that fluorescence response was influenced by GQD concentration, buffer conditions, and environmental pH, with suitable sensing performance observed at 0.50 mM GQD concentration and pH 7.2 phosphate buffer conditions. Under optimized experimental conditions, the smartphone-assisted RGB analysis demonstrated a concentration-dependent fluorescence response toward histamine within the tested concentration range of 0.00 - 0.75 mM. In addition, interference experiments showed that sodium and magnesium ions caused minimal fluorescence variation even at elevated concentration ratios, suggesting satisfactory selectivity and stability of the proposed sensing platform under conditions relevant to food analysis applications [7,11,29].

The integration of fluorescence-responsive GQDs with smartphone-based RGB image analysis and a 3D-printed optical enclosure demonstrates the potential of the proposed platform as a low-cost and portable preliminary screening tool for food safety monitoring. Compared with conventional laboratory-based instrumentation, the developed approach offers advantages in terms of operational simplicity, portability, and accessibility for rapid onsite analysis. Nevertheless, the present platform should currently be regarded as a proof-of-concept fluorescence sensing system rather than a replacement for standard confirmatory analytical methods such as HPLC [6,8,35].

Overall, this work contributes to the growing development of smartphone-assisted fluorescence sensing technologies for decentralized analytical applications. Future studies should focus on replicate validation, real food sample analysis, long-term stability evaluation, and further optimization of fluorescence sensitivity and selectivity to improve the practical applicability of the developed sensing platform [11,31,39].

Acknowledgements

The authors gratefully acknowledge the financial support provided by the Fundamental Fund 2025 (Fiscal Year 2568), which supported the completion of this research. The authors also thank the Department of Chemistry, Faculty of Science, Maejo University, Thailand for providing laboratory facilities and technical assistance. In addition, the authors acknowledge the Faculty of Pharmacy, Chiang Mai University, Thailand for instrumentation support and valuable scientific discussions that contributed to this study.

Declaration of generative AI in scientific writing

Generative AI tools were used solely for language refinement, grammar correction, and improvement of manuscript readability. All scientific interpretations, experimental results, and conclusions were developed and verified by the authors. The authors remain fully responsible for the content of this manuscript.

CRediT author statement

Kittichai Jinachai: Conceptualization, Methodology, Investigation, Formal analysis, Writing - original draft, Writing - review & editing, Supervision, and Project administration. **Jirapatpong Senabut:** Conceptualization, Investigation, Formal analysis, Data curation, Funding acquisition, Writing - original draft, and Writing - review & editing. **Anusorn Yodjaiphet:** Conceptualization, Investigation, Formal analysis, Data curation, and Writing - original draft. **Sakchai Satienperakul:** Conceptualization, Investigation, Formal analysis, Data curation, and Writing - original draft. **Mathukorn Sainakham:** Methodology, Visualization, Formal analysis, Data curation, Supervision, Writing - original draft, and Writing - review & editing.

References

[1] KP Rai, HR Pradhan, BK Sharma and SK Rijal. Histamine in foods: Its safety and human health implications. *Journal of Food Science and Technology Nepal* 2013; **8**, 1-11.

[2] A Halász, Á Baráth, L Simon-Sarkadi and W Holzapfel. Biogenic amines and their production by microorganisms in food. *Trends in Food Science & Technology* 1994; **5(2)**, 42-49.

[3] AR Shalaby. Significance of biogenic amines to food safety and human health. *Food Research International* 1996; **29(7)**, 675-690.

[4] JM Hungerford. Scombroid poisoning: A review. *Toxicon* 2010; **56(2)**, 231-243.

[5] P Visciano, M Schirone, R Tofalo and G Suzzi. Biogenic amines in raw and processed seafood. *Frontiers in Microbiology* 2012; **3**, 188.

[6] A Önal. A review: Current analytical methods for the determination of biogenic amines in foods. *Food Chemistry* 2007; **103(4)**, 1475-1486.

[7] R Shi, S Feng, CY Park, KY Park, J Song, JP Park, HS Chun and TJ Park. Fluorescence detection of histamine based on specific binding bioreceptors and carbon quantum dots. *Biosensors and Bioelectronics* 2020; **167**, 112519.

[8] G Rateni, P Dario and F Cavallo. Smartphone-based food diagnostic technologies: A review. *Sensors* 2017; **17(6)**, 1453.

[9] M Li, T Chen, JJ Gooding and J Liu. Review of carbon and graphene quantum dots for sensing. *ACS Sensors* 2019; **4(7)**, 1732-1748.

[10] MJ Molaei. Principles, mechanisms, and application of carbon quantum dots in sensors: A review. *Analytical Methods* 2020; **12(10)**, 1266-1287.

[11] G Wu, X Dou, D Li, S Xu, J Zhang, Z Ding and J Xie. Recent progress of fluorescence sensors for histamine in foods. *Biosensors* 2022; **12(3)**, 161.

[12] SN Baker and GA Baker. Luminescent carbon nanodots: Emergent nanolights. *Angewandte Chemie International Edition* 2010; **49(38)**, 6726-6744.

[13] S Zhu, Q Meng, L Wang, J Zhang, Y Song, H Jin, K Zhang, H Sun, H Wang and B Yang. Highly photoluminescent carbon dots for multicolor patterning, sensors, and bioimaging. *Angewandte Chemie International Edition* 2013; **52(14)**, 3953-3957.

[14] Z Huang and L Ren. Large scale synthesis of carbon dots and their applications: A review. *Molecules* 2025; **30(4)**, 774.

[15] P Dubey. An overview on animal/human biomass-derived carbon dots for optical sensing and bioimaging applications. *RSC Advances* 2023; **13(50)**, 35088-35126.

[16] TB Leta, JO Adeyemi and OA Fawole. Carbon dot nanoparticles synthesized from horticultural extracts for postharvest shelf-life extension of fruits and vegetables. *Plants* 2025; **14(16)**, 2523.

[17] NK Khairol Anuar, HL Tan, YP Lim, MS So'aib and NF Abu Bakar. A review on multifunctional carbon-dots synthesized from biomass waste: Design/fabrication, characterization and applications. *Frontiers in Energy Research* 2021; **9**, 626549.

[18] H Li, Z Kang, Y Liu and ST Lee. Carbon nanodots: Synthesis, properties and applications. *Journal of Materials Chemistry* 2012; **22(46)**, 24230-24253.

[19] YP Sun, B Zhou, Y Lin, W Wang, KS Fernando, P Pathak, MJ Meziani, BA Harruff, X Wang and H Wang. Quantum-sized carbon dots for bright and colorful photoluminescence. *Journal of the American Chemical Society* 2006; **128(24)**, 7756-7757.

[20] Y Qin, P Huang and FY Wu. Histamine-responsive dye-incorporated carbon dots for visual monitoring of food spoilage. *Sensors and Actuators B: Chemical* 2022; **365**, 131911.

[21] Y Dong, H Pang, HB Yang, C Guo, J Shao, Y Chi, CM Li and T Yu. Carbon-based dots co-doped with nitrogen and sulfur for high quantum yield and excitation-independent emission. *Angewandte Chemie International Edition* 2013; **52(30)**, 7800-7804.

[22] J Liu and Y Cao. An electrochemical sensor based on an anti-fouling membrane for the determination of histamine in fish samples. *Analytical Methods* 2021; **13(5)**, 685-694.

[23] R Liu, D Wu, S Liu, K Koynov, W Knoll and Q Li. An aqueous route to multicolor photoluminescent carbon dots using silica spheres as carriers. *Angewandte Chemie International Edition* 2009; **48(25)**, 4598-4601.

[24] ZL Wu, P Zhang, MX Gao, CF Liu, W Wang, F Leng and CZ Huang. One-pot hydrothermal synthesis of highly luminescent nitrogen-doped amphoteric carbon dots for bioimaging from Bombyx mori silk-natural proteins. *Journal of Materials Chemistry B* 2013; **1(22)**, 2868-2873.

[25] X Li, M Rui, J Song, Z Shen and H Zeng. Carbon and graphene quantum dots for optoelectronic and energy devices: A review. *Advanced Functional Materials* 2015; **25(31)**, 4929-4947.

[26] Y Dong, J Shao, C Chen, H Li, R Wang, Y Chi, X Lin and G Chen. Blue luminescent graphene quantum dots and graphene oxide prepared by tuning the carbonization degree of citric acid. *Carbon* 2012; **50(12)**, 4738-4743.

[27] S Qu, X Wang, Q Lu, X Liu and L Wang. A biocompatible fluorescent ink based on water-soluble luminescent carbon nanodots. *Angewandte Chemie International Edition* 2012; **51(49)**, 12215-12218.

[28] Q Li, B Chen and B Xing. Aggregation kinetics and self-assembly mechanisms of graphene quantum dots in aqueous solutions: Cooperative effects of pH and electrolytes. *Environmental Science & Technology* 2017; **51(3)**, 1364-1376.

[29] C Li, A Hassan, M Palmai, P Snee, PC Baveye and CJ Darnault. Colloidal stability and aggregation kinetics of nanocrystal CdSe/ZnS quantum dots in aqueous systems: Effects of ionic strength, electrolyte type, and natural organic matter. *SN Applied Sciences* 2022; **4(4)**, 101.

[30] A Maity, D Bagchi, H Tabassum, P Nath, S Sinha and A Chakraborty. Diverse role of buffer mediums and protein concentrations to mediate the multimodal interaction of phenylalanine-functionalized gold nanoparticle and lysozyme protein at same nominal pH. *The Journal of Physical Chemistry B* 2024; **128(43)**, 10625-10635.

[31] X Zhang, M Asif, A Aziz, J Wang, X Sun, R Zhao, R Wang, C Dong and S Shuang. Dual fluorophores embedded into zeolitic imidazolate framework-8 for ratiometric fluorescence monitoring of pH and histamine in seafood samples and bioimaging. *Talanta* 2026; **296**, 128476.

[32] AS El-Shafie, S Hassan, S Al-Meer, K Al-Saad and M El-Azazy. Smart fluorescence graphene quantum dot-based on-off sensor for tracing antibiotic residues in milk. *Emergent Materials* 2025; **8(7)**, 5643-5658.

[33] MSA Ja'farawy, D Thirumalai, J Lee, HS Jung, SC Chang, JH Yoon and DH Kim. Graphene quantum dot nanocomposites: Electroanalytical and optical sensor technology perspective. *Journal of Analytical Science and Technology* 2023; **14(1)**, 29.

[34] T Krishnan, HN Wang and T Vo-Dinh. Smartphone-based device for colorimetric detection of MicroRNA biomarkers using nanoparticle-based assay. *Sensors* 2021; **21(23)**, 8044.

[35] L Ciaccheri, B Adinolfi, AA Mencaglia and AG Mignani. Smartphone-enabled colorimetry. *Sensors* 2023; **23(12)**, 5559.

[36] MA Hossain and J Canning. Developments and drivers of low-cost smartphone instrumentation. *Advanced Devices & Instrumentation* 2024; **5**, 0068.

[37] L Shen, JA Hagen and I Papautsky. Point-of-care colorimetric detection with a smartphone. *Lab on A Chip* 2012; **12(21)**, 4240-4243.

[38] B Coleman, C Coarsey and W Asghar. Cell phone based colorimetric analysis for point-of-care settings. *Analyst* 2019; **144(6)**, 1935-1947.

[39] M Vargas-Muñoz, J Morales, V Cerdà, L Ferrer and E Palacio. Paper sensor-based method using a portable 3D-printed platform and smartphone-assisted colorimetric detection for ammonia and sulfide monitoring in anaerobic digesters and wastewater. *Microchemical Journal* 2023; **188**, 108469.

[40] SD Kim, Y Koo and Y Yun. A smartphone-based automatic measurement method for colorimetric pH detection using a color adaptation algorithm. *Sensors* 2017; **17(7)**, 1604.

[41] ZY Gündüz, C Gündüz, C Özpınar and OA Urucu. A novel Schiff-base as a Cu (II) ion fluorescent sensor in aqueous solution. *Spectrochimica Acta Part A: Molecular and Biomolecular Spectroscopy* 2015; **136**, 1679-1683.

[42] L Wang, X Ran, H Tang and D Cao. Recent advances on reaction-based amine fluorescent probes. *Dyes and Pigments* 2021; **194**, 109634.

[43] KS Keremane, MG Acharya, P Naik, CC Malakar, K Wang and B Poudel. Recent advances in aggregation-induced emission (AIE) fluorescent sensors for biomolecule detection. *Chemosensors* 2025; **13(5)**, 174.